Architecture of Rod–Brush Block Copolymers Synthesized by a Combination of Coordination Polymerization and Atom Transfer Radical Polymerization

Koji Ishizu, Naomasa Hatoyama, Satoshi Uchida

Department of Organic Materials and Macromolecules, International Research Center of Macromolecular Science, Tokyo Institute of Technology, 2-12-1-H-133, Ookayama, Meguro-ku, Tokyo 152-8552, Japan

ABSTRACT: A combination of coordination polymerization and atom transfer radical polymerization (ATRP) was applied to a novel synthesis of rod–brush block copolymers. The procedure included the following steps: (1) the monoesterification reaction of ethylene glycol with 2-bromoisobutyryl bromide (BIBB) yielded the bifunctional initiator monobromobutyryloxy ethylene glycol and (2) a trichlorocyclopentadienyl titanium (CpTiCl$_3$; bifunctional initiator) catalyst was prepared from a mixture of CpTiCl$_3$ and bifunctional initiator. The coordination polymerization of *n*-butyl isocyanate initiated by such a catalyst provided a well-defined macroinitiator, poly(*n*-butyl isocyanate)–bromine (PBIC–Br). (3) The ATRP method of 2-hydroxyethyl methacrylate initiated by PBIC–Br provided rod [poly(*n*-butyl isocyanate) (PBIC)]–coil [poly(2-hydroxyethyl methacrylate) (PHEMA)] block copolymers with a CuCl/CuCl$_2$/2,2′-bipyridyl catalyst. (4) The esterfication of PBIC-*block*-PHEMA with BIBB yielded a block-type macroinitiator, and (5) ATRP of methyl methacrylate with a block-type macroinitiator provided rod–brush block copolymers. We found from the solution properties that such rod–brush block copolymers formed nanostructured macromolecules in solution. © 2008 Wiley Periodicals, Inc. J Appl Polym Sci 108: 3346–3352, 2008

Key words: atom transfer radical polymerization (ATRP); rod-brush block copolymer; coordination polymerization; nanostructured polymer

INTRODUCTION

The variation of molecular architecture has become an increasingly important tool in the search for materials with excellent properties. Polyisocyanates (PICs) are an unusual class of polymeric materials that adopt a helical conformation both in solution and in bulk.[1–5] Numerous characterization techniques have shown that PIC is made of stiff-chain polymers whose properties depend on several parameters, such as the nature of the isocyanate side group, temperature, solvent, and molecular weight.[6,7] Consequently, they may behave either as rigid rods or as semiflexible, wormlike chains.

On the other hand, there has been rapid growth in the number of techniques used in the area of controlled/living radical polymerization, such as atom transfer radical polymerization (ATRP),[8,9] nitroxide-mediated radicals,[10] and reversible addition–fragmentation chain transfer polymerization.[11–14] Until recently, ionic polymerizations (anionic or cationic) were the only living technique available that efficiently controlled the structure and architecture of vinyl polymers. Although these techniques ensure low-polydispersity materials with controlled molecular weights and defined chain ends, they are not useful for certain polymerizations and copolymerizations of functionalized vinyl monomers. More recently, we explored the scope of the synthetic approach to the creation of rod–coil block copolymers with a combination of the coordination polymerization of *n*-butyl isocyanate (BIC) and ATRP of vinyl monomers [styrene and methyl methacrylate (MMA)].[15] It is well known that comb polymers with densely grafted side chains in a good solvent can adopt wormlike cylinder brush conformations in which the side chains are stretched in the direction normal to the backbone because of the excluded volume interaction. Usually, two strategies can be designed to construct such structures. The polymerization of macromonomers provides regular multi-branched polymers with dense branching. Polymacromonomers, often so-called polymer brushes, are interesting models for the study of branched polymers. As another synthetic strategy reported by Matyjaszewski's et al.,[16] the grafting-from ATRP is a nice approach for the architecture of polymer

Correspondence to: K. Ishizu (kishizu@polymer.titech.ac.jp).
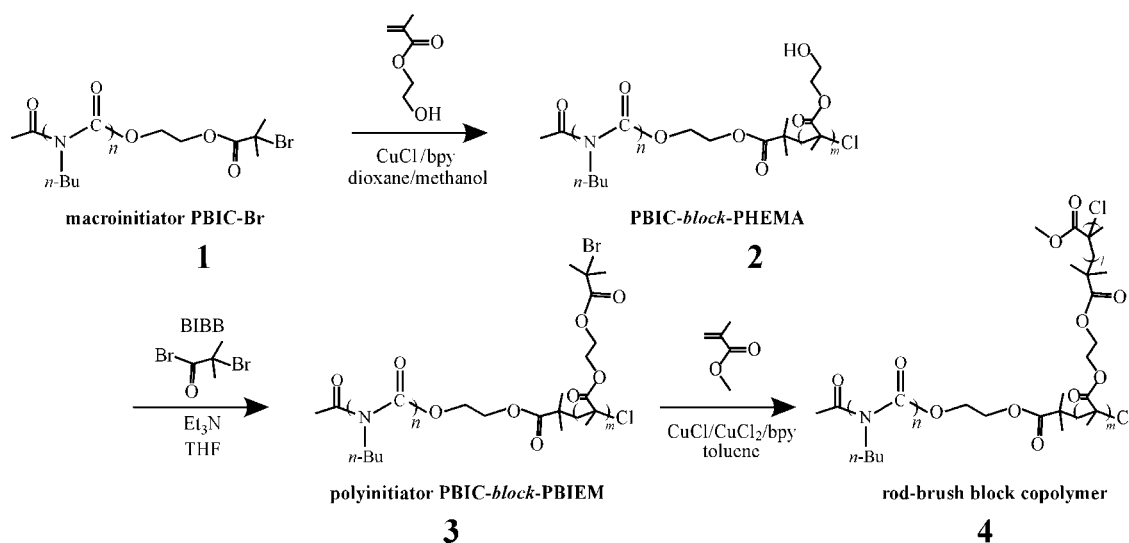
Scheme 1 Synthesis route for rod–brush block copolymers.

brushes. More recently, we reported the architecture of prototype copolymer brushes by the grafting-from ATRP approach.[17] In short, the free-radical copolymerization of vinylbenzyl-terminated polystyrene macromonomer and N-(4-hydroxyphenyl)maleimide gave well-defined alternating comb-shaped copolymers. The subsequent esterification of such comb-shaped copolymers with 2-bromoisobutyryl bromide (BIBB) yielded a comb-shaped macroinitiator. The grafting-from ATRP approach from functionalized alternating comb-shaped macroinitiators is a new route for the construction of prototype copolymer brushes. This synthetic strategy can be applied to the preparation of rod–brush copolymers.

In this article, we discuss the novel synthesis of rod–brush block copolymers by the grafting-from ATRP approach from rod–coil block copolymers, where the poly(2-hydroxyethyl methacrylate) (PHEMA) coil block had functionalized pendant Br groups. The procedure included the following steps: (1) a combination of coordination polymerization and ATRP provided rod (PIC)–coil (PHEMA) block copolymers, (2) a subsequent esterification reaction of such block copolymers with BIBB yielded a block-type macroinitiator, and (3) the grafting-from ATRP method of MMA with a block-type macroinitiator provided PIC–poly(methyl methacrylate) (PMMA) rod–brush block copolymers.

EXPERIMENTAL

Materials

BIC (Tokyo Kasei Organic Chemicals, Tokyo) was dried over calcium hydride (CaH$_2$) and distilled in vacuo. 2-Hydroxyethyl methacrylate (HEMA) and MMA (Tokyo Kasei Organic Chemicals, Tokyo) were

distilled in vacuo. BIBB, ethylene glycol, triethyl amine (Et$_3$N), 2,2′-bipyridyl (bpy), tetrahydrofuran (THF), dioxane, chloroform (CHCl$_3$), n-hexane, methanol (Tokyo Kasei Organic Chemicals, Tokyo), trichlorocyclopentadienyl titanium (CpTiCl$_3$), basic aluminum oxide (Aldrich, Milwaukee, WI), CaH$_2$, copper(I) chloride (CuCl), CuCl$_2$, and hydrochloric acid (HCl; Kanto Reagent Division, Tokyo) were used as received.

Synthesis of the rod–coil block copolymers (2) by ATRP

Scheme 1 shows the synthesis routes of the rod–brush block copolymers. A poly(n-butyl isocyanate) (PBIC) macroinitiator, poly(n-butyl isocyanate)–bromine (PBIC–Br or **1**) was prepared by the coordination polymerization of BIC. The details concerning the synthesis and characterization of **1** were given elsewhere.[15] In brief, the bifunctional initiator, monobromobutyryloxy ethylene glycol, was synthesized by the reaction of ethylene glycol and BIBB in THF. The PBIC–Br macroinitiator (**1**) was prepared by the coordination polymerization of BIC initiated by the complex catalyst CpTiCl$_3$ and monobromobutyryloxy ethylene glycol (1:1 molar ratio) in THF.

ATRP operations for the block copolymer synthesis were carried out in a sealed glass apparatus with high-vacuum techniques (degassed polymerization mixture). Typical polymerization conditions for the synthesis of PBIC-block-PHEMA [code PBIC$_{35}$–PHEMA$_{69}$, where the subscript indicates the degree of polymerization (DP$_n$) of each block] are as follows. PBIC$_{35}$–Br (0.29 g, 0.08 mmol), HEMA (1.07 g, 8 mmol), CuCl (7.9 mg, 0.08 mmol), CuCl$_2$ (0.2 mg, 0.0016 mmol), and bpy (38.4 mg, 0.24 mmol; [PBIC$_{62}$–Br]/[HEMA]/[CuCl]/[CuCl$_2$]/[bpy]

= 1 : 100 : 1 : 0.2 : 3) were dissolved in dioxane/methanol (4/1 v/v; 1.4 mL; 33 vol % monomer solution), and the resulting mixture was stirred at room temperature for 1 h to form a copper complex, CuCl/bpy. After ATRP polymerization at 40°C for 5 h, the crude product was recovered by precipitation in *n*-hexane. The final polymerization mixture was diluted with THF, the solution was filtered through a column filled with basic aluminum oxide to remove the catalyst, and the polymer was precipitated in an excess of *n*-hexane and dried *in vacuo* to a constant weight (conversion of HEMA = 6%).

Synthesis of the block-type macroinitiators (3)

The initiating sites (Br groups) were introduced by the esterification of the PHEMA coil block with BIBB. Typical reaction conditions were as follows. A mixture of $PBIC_{67}$–$PHEMA_{92}$ (2; 0.3 g), BIBB (1 mL, excess amount to the OH groups of the PHEMA block), and Et_3N (BIBB/Et_3N = 1 : 1.3 molar ratio) as an acid acceptor was stirred in THF (8 mL) for 3 h at 0°C; it was then stirred at 40°C for 5 days. The resulting solution was placed in dialysis tubes and dialyzed against distilled water for 4 days to remove the catalyst and unreacted BIBB. The solvent was evaporated and PBIC-*block*-poly[2-(2-bromobutyryloxy)ethyl methacrylate] (PBIEM) macroinitiator was precipitated from the THF solution to *n*-hexane.

Preparation of the rod–brush block copolymers (4) by ATRP

Typical polymerization conditions for the synthesis of the rod–brush block copolymers (4) were as follows. The block-type macroinitiator, $PBIC_{67}$–$PBIEM_{92}$ (37 mg, 0.19 mmol), MMA (1.87 g, 18.7 mmol), CuCl (18.8 mg, 0.19 mmol), and bpy (0.89 g, 0.57 mmol; [Br]/[MMA]/[CuCl]/[bpy] = 1 : 100 : 1 : 3, where [Br] indicates the Br concentration of pendant Br groups of the PBIEM block) were dissolved in toluene (4 mL; 33 vol % monomer solution), and the resulting mixture was stirred at room temperature for 1 h to form a copper complex, CuCl/bpy. After ATRP polymerization at 40°C for 2.5 h, the crude product was recovered by precipitation in methanol containing dilute HCl to remove roughly the copper complex. The final polymerization mixture was diluted with THF, the solution was filtered through a column filled with basic aluminum oxide to remove the catalyst, and the polymer was precipitated in an excess of methanol and dried *in vacuo* to a constant weight (conversion of MMA = 11%).

Characterization

The polydispersities [weight-average molecular weight/number-average molecular weight (M_w/M_n)] of the PBIC–Br macroinitiator (1), block-type macroinitiator (3), and rod–brush block copolymers (4) were determined by gel permeation chromatography (GPC; HLC-8120 high-speed liquid chromatograph, Tosoh, Tokyo) with two TSK gel columns, GMH_{XL} [excluded-limit molecular weight (M_{ELM}) = 4 × 10^8] and $G2000H_{XL}$ (M_{ELM} = 1 × 10^4) in series in THF as the eluent (flow rate = 1.0 mL/min) at 40°C with PS standard samples. M_n of 3 was determined by the integration ratio of methylene protons (a; δ 3.70 ppm) adjacent to N of PBIC to ethylene protons (g; 4.37 ppm) of the PBIEM block from proton nuclear magnetic resonance (^{1}H-NMR) spectra. ^{1}H-NMR spectroscopy (300 MHz, Bruker GPX300 NMR spectrometer, Germany) for 3 and 4 was performed in $CDCl_3$. M_w of the rod–brush block copolymer (4) was determined by static light scattering (SLS; Photal DLS-8000PNA, Otsuka Electronics, Tokyo, He–Ne laser λ_0 = 632.8 nm, 10 mW) with Zimm mode in $CHCl_3$ (n_D = 1.444, viscosity = 0.542 cP) at 25°C. The refractive-index increment of 4 was determined by a differential refractometer (Photal DRM-1021, Tokyo; λ_0 = 632.8 nm). Sample solutions were filtered through membrane filters with a nominal pore of 0.2 μm just before measurement. The translational diffusion coefficient (D_0) was determined by extrapolation to zero concentration on dynamic light scattering (DLS; Otsuka Electronics) data with the cumulant method at 25°C in 2–10 mg/mL $CHCl_3$ solution of 4. The scattering angle was in the range 30–150°.

The morphological behavior of the rod–brush block copolymers was obtained as follows. A THF solution of 0.1 wt % concentration was dropped on a microscope mesh coated with carbon film to perform transmission electron microscopy (TEM). The specimen was sputtered with Pd–Pt at a 20° tilt angle. The morphological results were obtained on a Hitachi H-500 transmission electron microscope (Tokyo) at 100 kV.

RESULTS AND DISCUSSION

Preparation of the rod–coil block copolymers and block-type macroinitiators

As mentioned in the previous article,[15] PBIC–Br macroinitiators could be controlled roughly by the feed ratio of [BIC]/[Ti complex] and [$CpTiCl_3$] initiator concentration in the coordination polymerization. It is well known for the block copolymer synthesis that the poly(methacrylate) macroinitiator, having a bromine atom at the end group, effectively initiates the ATRP of methacrylate monomers in the presence of the catalyst CuCl; that is, a halide exchange should take place.[18–20] Therefore, we performed a halide exchange equilibrium to achieve a narrow

TABLE I
Polymerization Conditions and Results for the PBIC-*block*-PHEMA Block Copolymers[a]

Code	[PBIC–Br] (mmol)[b]	[PBIC–Br]: [HEMA]:[CuCl]: [CuCl$_2$]:[bpy]	Time (h)	Conversion (%)[c]	10^{-4} M_n[d]	DP$_{n,\text{PHEMA}}$[e]	Theoretical DP$_{n,\text{PHEMA}}$[f]	M_w/M_n[g]
PBIC$_{62}$–PHEMA$_{92}$	0.25	1 : 100 : 1 : 0 : 3	1	30	1.81	92	30	1.32
PBIC$_{33}$–PHEMA$_{117}$	0.12	1 : 100 : 1 : 0 : 3	1	20	1.89	117	20	1.31
PBIC$_{35}$–PHEMA$_{69}$	0.08	1 : 100 : 1 : 0.2 : 3	5	6	1.06	69	6	1.19
PBIC$_{35}$–PHEMA$_{104}$	0.08	1 : 100 : 1 : 0.1 : 3	5	15	1.09	104	15	1.20

[a] The polymerizations were performed in 4/1 (v/v) dioxane/methanol at 40°C (33 vol % monomer solution).
[b] The polydispersity of the macroinitiators was 1.15 for PBIC$_{33}$–Br, 1.18 for PBIC$_{35}$–Br, and 1.23 for PBIC$_{62}$–Br.
[c] The conversion was determined by the gravimetric method.
[d] Determined from M_n of PBIC–Br and the composition of the block copolymers.
[e] Determined by ^{1}H-NMR spectra in CDCl$_3$.
[f] The theoretical DP$_n$ (theoretical DP$_{n,\text{PS}}$) was calculated under the assumption that one molecule of the macroinitiator generated one polymer chain and the initiator efficiency was unity. DP$_{n,\text{PS}}$ is degree of polymerization of PS.
[g] Determined by GPC of PBIC-*block*-PBIEM in THF as an eluent at 40°C with the calibration of PS standard samples.

polydispersity for the PBIC-*block*-PMMA synthesis initiated by PBIC–Br with CuCl in the ATRP method instead of CuBr. Then, PBIC-*block*–PHEMA was prepared in accordance with the previous reference. The polymerization conditions and results of PBIC-*block*-PHEMA are listed in Table I. We could not carry out the GPC measurements for the PBIC-*block*-PHEMA block copolymers because such block copolymers produced were soluble heterogeneously in THF. Then, PBIC-*block*-PHEMA was derived to PBIC-*block*-PBIEM by esterification with BIBB. We carried out following characterizations because the PBIC-*block*-PBIEM macroinitiators were soluble in THF.

Figure 1(a) shows a typical ^{1}H-NMR spectrum of PBIC$_{62}$–PBIEM$_{92}$ in CDCl$_3$. The strong peaks at δ 0.92 ppm (d), 1.32 ppm (c), 1.61 ppm (b), and 3.70 ppm (a) were assignable to the methyl (d), methylene (c,b), and methylene (a) adjacent to N of the *n*-butyl groups of the PBIC block, respectively. The characteristic peaks observed at 4.37 ppm (g) and 4.20 ppm (h), 1.08 ppm (f; this peak overlapped partially with the signal of d), 1.97 ppm (i), and 1.84 ppm (e) were assignable to the methylene (g,h), α-methyl (f), methyl (i; bromobutyryloxy group), and methylene (e) protons of the PBIEM pendant chain and backbone, respectively. The signal intensity ratio [f:i, where f/(d + f) = 92/154] was estimated to be 1:2 within experimental error. This means that the esterification proceeded quantitatively in these reaction conditions. The composition of the PBIEM block (59.7 mol %) was estimated from the signal intensity of the methylene protons (g) of PBIEM to the methylene protons (a) of PBIC. A typical GPC profile of block-type macroinitiator PBIC$_{62}$–PBIEM$_{92}$ is shown in Figure 2. The GPC curve of PBIC$_{62}$–PBIEM$_{92}$ had a monomodal molecular weight distribution and shifted to the high-molecular-weight side compared with that of the PBIC$_{62}$–Br precursor (M_w/M_n = 1.23). PBIC$_{62}$–PBIEM$_{92}$ had a relatively narrow molecular

weight distribution (M_w/M_n = 1.32). Halide exchange contributed to an increase in the relative rate of initiation to propagation. However, the DP$_{n,\text{PHEMA}}$ (equal to DP$_{n,\text{PBIEM}}$) values for PBIC$_{62}$–PHEMA$_{92}$ and PBIC$_{33}$–PHEMA$_{117}$ were much larger than the theoretical DP$_{n,\text{PHEMA}}$ values (see Table I).
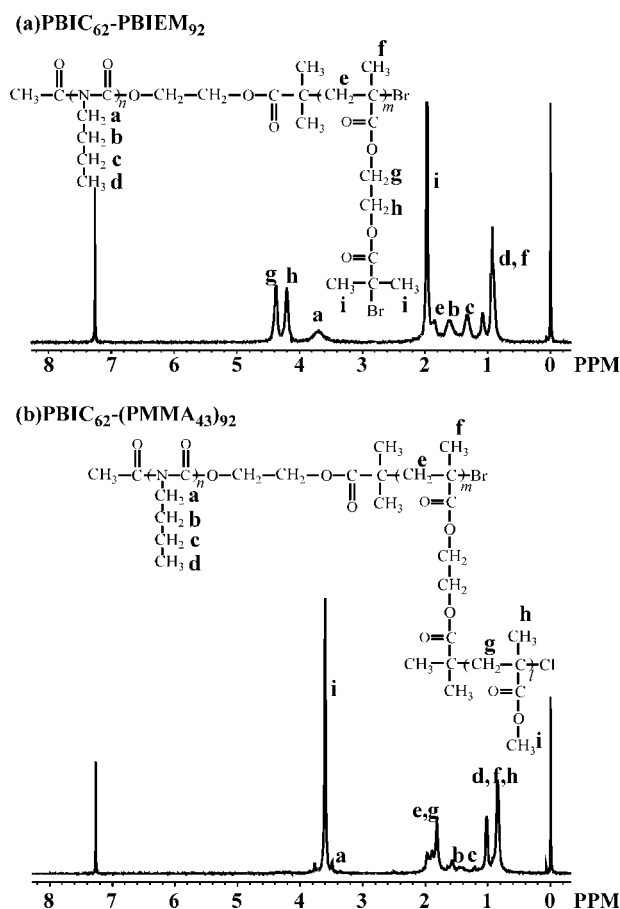
Figure 1 ^{1}H-NMR spectra of (a) block-type macroinitiator PBIC$_{62}$–PBIEM$_{92}$ and (b) rod–brush block copolymer PBIC$_{62}$–(PMMA$_{43}$)$_{92}$ in CDCl$_3$.
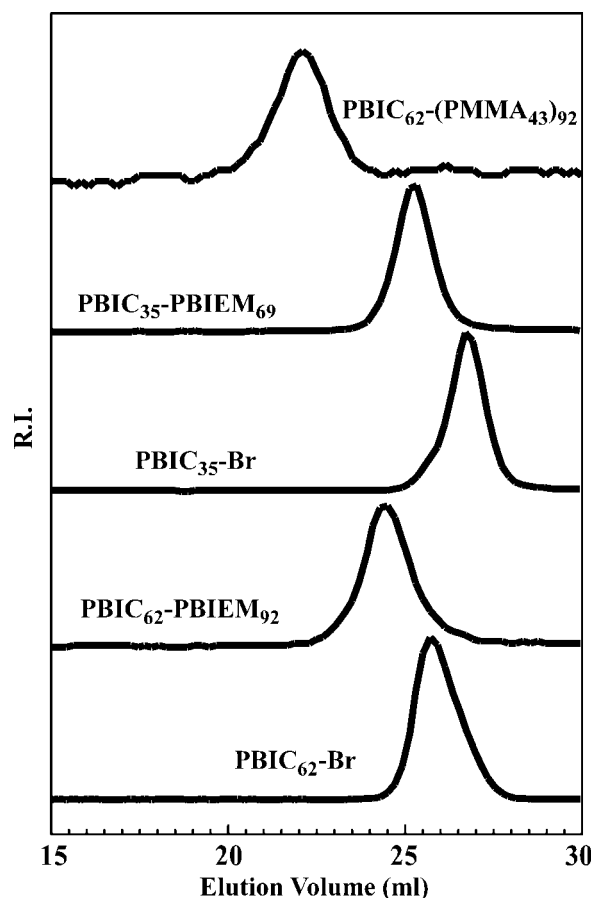
Figure 2 GPC profiles of macroinitiators PBIC$_{35}$–Br and PBIC$_{62}$–Br, block-type macroinitiators PBIC$_{62}$–PBIEM$_{92}$ and PBIC$_{35}$–PBIEM$_{69}$, and rod–brush block copolymer PBIC$_{62}$–(PMMA$_{43}$)$_{92}$ in THF as an eluent at 40°C. RI is the refractive index.

In the case of high reactive monomers such as HEMA, a less active catalyst must be used to reduce termination reactions.[21] We used the CuCl/CuCl$_2$/bpy catalyst for PBIC$_{35}$–PHEMA$_{69}$ and PBIC$_{35}$–PHEMA$_{104}$ (see Table I). A typical GPC profile of the esterification product PBIC$_{35}$–PBIEM$_{69}$ is also shown in Figure 2. This GPC distribution had a single and narrow molecular weight distribution (M_w/M_n = 1.19) and shifted completely to the high-molecular-weight side compared with that of the PBIC$_{35}$–Br precursor (M_w/M_n = 1.18). The conversion of HEMA was 6% after 5 h of reaction time, and the reaction rate was very slow compared with the reaction system in the absence of CuCl$_2$ (PBIC$_{62}$–PHEMA$_{92}$ and PBIC$_{33}$–PHEMA$_{117}$; HEMA conversion = 30–20%). However, molecular weight control of the PHEMA blocks could not be achieved in these systems. PBIC$_{35}$–PHEMA$_{104}$ showed also similar results. The heterogeneous solution system may have been the direct cause because we could not find a common solvent for both the PBIC and PHEMA segments. It would be better to use a protected monomer of HEMA such as 2-(trimethylsilyloxy) ethyl methacrylate[21] in this ATRP system.

Preparation of the rod–brush block copolymers by grafting-from ATRP

Table II lists the polymerization conditions and results for the rod–brush block copolymers prepared by the grafting-from ATRP approach. The polymerizations were quenched under relatively low conversion (ca. 10%) to avoid gelation due to intermolecular radical couplings. Figure 2 also shows the GPC profile of the rod–brush block copolymer PBIC$_{62}$–(PMMA$_{43}$)$_{92}$. The GPC curve of PBIC$_{62}$–(PMMA$_{43}$)$_{92}$ shifted to the high-molecular-weight side compared with that of the PBIC–PBIEM$_{92}$ precursor, keeping not only a monomodal distribution but also almost the same polydispersity (M_w/M_n = 1.30). The ^{1}H-NMR spectrum also gave support to the rod–brush copolymer formed [see Fig. 1(b)]. The spectrum displayed the expected resonances for the methyl (d) and methylene (a–c) protons of PBIC and the methoxy protons (i; δ 3.60 ppm) and α-methyl protons (h) of the PMMA grafted chains. The composi-

TABLE II
Polymerization Conditions, Characteristics, and Solution Properties for the Rod–Brush Block Copolymers[a]

			Rod–brush block copolymer					
Code	[3] (mmol)[b]	[MMA] (mmol)	Conversion (%)[c]	10^{-5} M_w[d]	M_w/M_n[e]	DP$_{n,\text{PMMA}}$[f]	R_g (nm)[d]	R_h (nm)[g]
PBIC$_{62}$–(PMMA$_{43}$)$_{92}$	0.19	18.7	11	5.43	1.30	43	18.2	13.8
PBIC$_{33}$–(PMMA$_{45}$)$_{117}$	0.19	18.7	12	7.18	1.32	45	14.4	24.7

[a] The polymerizations were performed in toluene (4 mL; 33 vol % monomer solution) at 40°C for 2.5 h. The [**3**]/[MMA]/[CuCl]/[bpy] feed ratio was 1 : 100 : 1 : 3.
[b] PBIC$_{62}$–PBIEM$_{92}$ and PBIC$_{33}$–PBIEM$_{117}$ were used as block-type polyinitiators.
[c] The conversion was determined by the gravimetric method.
[d] Determined by SLS with the Zimm mode in CHCl$_3$ at 25°C.
[e] Determined by GPC in THF as an eluent at 40°C with the calibration of PS standard samples.
[f] Determined from M_n of the rod–brush block copolymer (converted from M_w and M_w/M_n) and the PBIC–Br macroinitiator.
[g] Determined by DLS with the cumulant method in CHCl$_3$ at 25°C.

tion of the rod–brush block copolymers was left out of the NMR signals due to the weak signals of the PBIC block. The characteristics of the rod–brush block copolymers are discussed next.

Characterization and solution properties of the rod–brush block copolymers

The characteristics of the rod–brush block copolymers are also listed in Table II. M_w and the radius of gyration (R_g) were determined by SLS data with the Zimm mode. For example, we calculated the degree of polymerization of the PMMA-grafted chains ($DP_{n,PMMA}$) to be 43 from both M_n of the rod–brush block copolymer $PBIC_{62}$–$(PMMA_{43})_{92}$ (converting from M_w and M_w/M_n of rod–brush block copolymer) and $PBIC_{62}$–Br macroinitiator, assuming that all of the initiation sites on the block-type macroinitiator led to the propagation of MMA. This value was very large compared with the theoretical $DP_{n,PMMA}$ value of 11 calculated from the feed ratio and conversion. The theoretical values of DP_n for $PBIC_{62}$–$(PMMA_{43})_{92}$ and $PBIC_{33}$–$(PMMA_{45})_{117}$ were much different from the experimental data, regardless of the lower polydispersity than each starting macroinitiator ($PBIC_{62}$–$PBIEM_{92}$ and $PBIC_{33}$–$PBIEM_{117}$; $M_w/M_n \approx 1.32$). The reason for this was not yet found. We concluded that the sample $PBIC_{62}$–$(PMMA_{43})_{92}$ had in total 62 chain units of rod block and 92 main chain units having 43 PMMA side-chain units of brush block. The physical values for $PBIC_{33}$–$(PMMA_{45})_{117}$ are also listed in Table II.

To discuss the geometrical anisotropy and intermolecular interaction, we determined D_0 of the rod–brush block copolymers. In general, the mutual diffusion coefficient [$D(C)$] is defined as $D(C) \equiv \Gamma_e q^{-2}_{\theta \to 0}$, where Γ_e, q, and θ are the first cumulant, scattering vector, and scattering angle, respectively. The angular dependences of $\Gamma_e q^{-2}$ ($qR_h < 1$, where R_h is the hydrodynamic radius) for $PBIC_{62}$–$(PMMA_{43})_{92}$ and $PBIC_{33}$–$(PMMA_{45})_{117}$ are shown in Figure 3(a). Both rod–brush copolymers showed weak angular dependences. The weak dependence of $\Gamma_e q^{-2}$ on q^2 showed that there was only a single diffusion mode. In general, polymer brushes composed of a long aspect ratio take the wormlike conformation in a good solvent.[22,23] However, these rod–brush copolymers were composed of brush with a short aspect ratio and a linear rod chain. Then, this macromolecule exhibited a tadpole-shaped structure in which a linear rod was connected to the brush head in solution.

Figure 3(b) shows the relationship between $D(C)$ and the polymer concentration for $PBIC_{62}$–$(PMMA_{43})_{92}$ and $PBIC_{33}$–$(PMMA_{45})_{117}$. Each $D(C)$ had an almost constant value in the range 2–10 mg/mL of polymer concentration. This suggests that these copolymers were molecularly dissolved in the
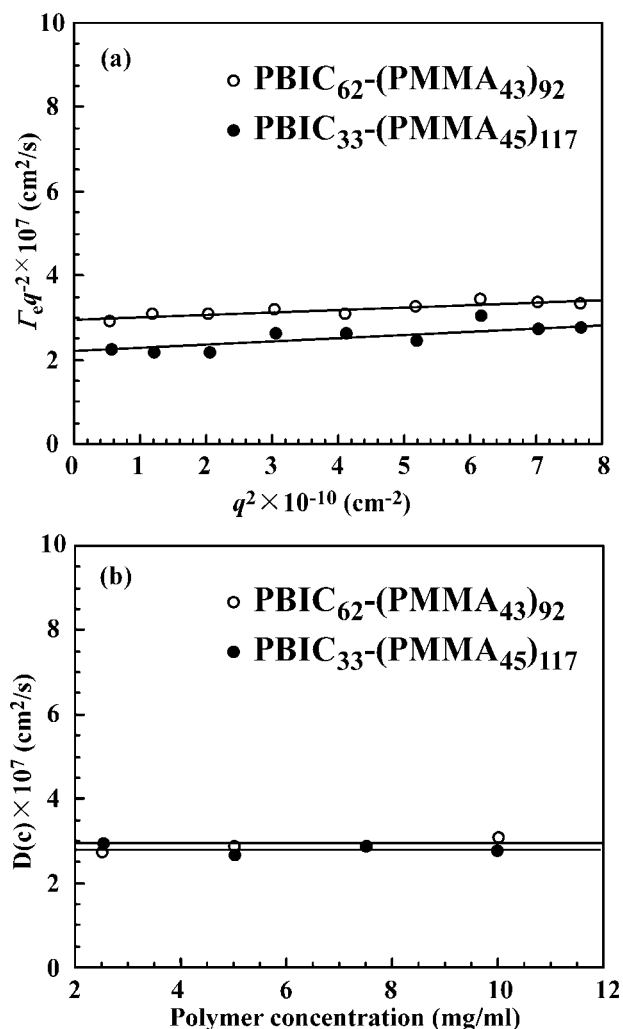

Figure 3 DLS data for rod–brush block copolymers $PBIC_{33}$–$(PMMA_{45})_{117}$ and $PBIC_{62}$–$(PMMA_{43})_{92}$ in $CHCl_3$ at 25°C: (a) $\Gamma_e q^{-2}$ versus q^2 and (b) $D(C)$ versus the polymer concentration.

dilute solution. D_0 could be estimated by the extrapolation of polymer concentration (C) to zero. R_h is defined by the Stokes–Einstein equation, $R_h = kT/6\pi\eta_0 D_0$, where k, T, and η_0 indicate the Boltzmann coefficient, absolute temperature, and viscosity of the solvent, respectively. For example, the values of D_0 and R_h for $PBIC_{62}$–$(PMMA_{43})_{92}$ were as follows: $D_0 = 2.3 \times 10^{-7}$ cm²/s and $R_h = 13.8$ nm.

Morphological behaviors of the rod–brush block copolymers

Figure 4(a,b) shows TEM photographs of the rod–brush block copolymers $PBIC_{62}$–$(PMMA_{43})_{92}$ and $PBIC_{33}$–$(PMMA_{45})_{117}$, respectively, sputtered with Pd–Pt at a 20° tilt angle. We found from these textures that spherical particles were visible clearly on the carbon substrate in both samples. For example, in Figure 4(a) [$PBIC_{62}$–$(PMMA_{43})_{92}$], the average par-
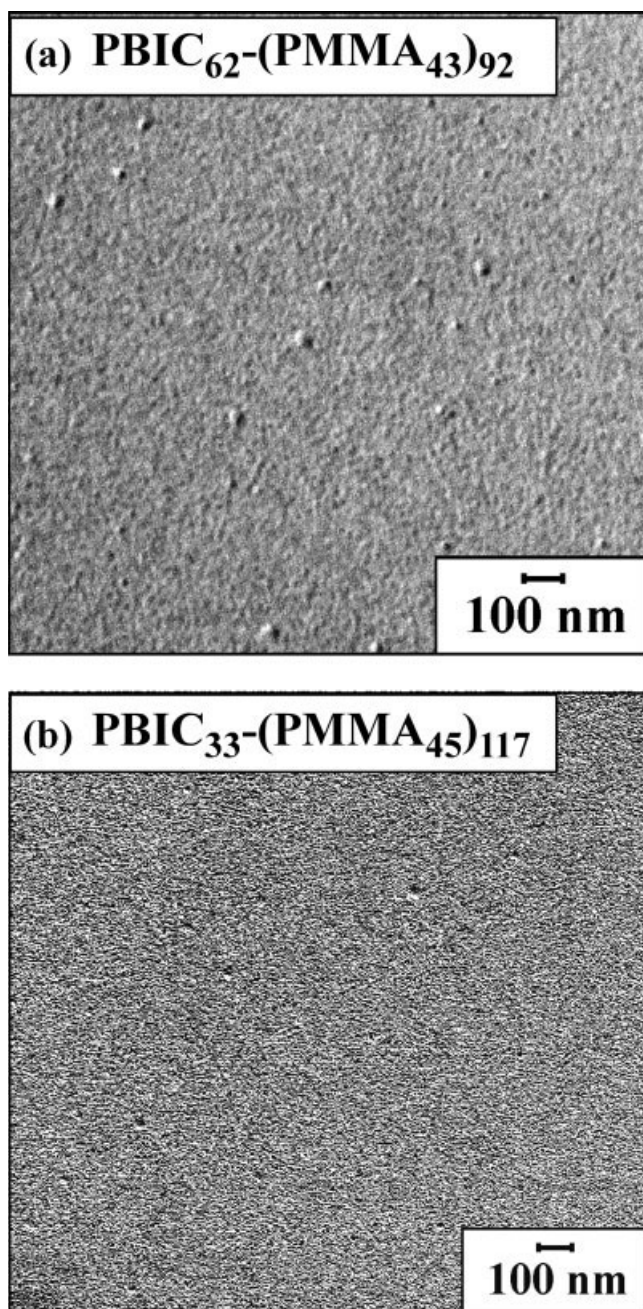
Figure 4 TEM photographs of rod–brush block copolymers sputtered with Pt–Pd at a tilt angle of 20°: (a) PBIC$_{62}$–(PMMA$_{43}$)$_{92}$ and (b) PBIC$_{33}$–(PMMA$_{45}$)$_{117}$.

ticle size and height were estimated to be 25 and 17.7 nm, respectively. The observed average particle size was somewhat small than R_h (27.6 nm; see Table II) in solution due to shrinkage in the solid state. The PBIC rod chain may have clung to the surface of a brush sphere in the solid state. The morphological results for PBIC$_{33}$–(PMMA$_{45}$)$_{117}$ also showed a similar trend. The materials obtained in this work will provide interesting information for micelle formation and microphase separation.

CONCLUSIONS

We explored the scope of a synthetic approach to the preparation of rod–brush block copolymers with a combination of the coordination polymerization of BIC and ATRP of vinyl monomers. Monodisperse PBIC-*block*-PHEMA block copolymers could be synthesized by ATRP of HEMA initiated by a PBIC–Br macroinitiator with the catalyst CuCl/CuCl$_2$/bpy. The subsequent esterification of such block copolymers with BIBB yielded a block-type macroinitiator, PBIC-*block*-PBIEM. The grafting-from ATRP approach from a block-type macroinitiator is a new route for constructing rod–brush block copolymers. Both PBIC$_{62}$–(PMMA$_{43}$)$_{92}$ and PBIC$_{33}$–(PMMA$_{45}$)$_{117}$, obtained in this study, exhibited a tadpole-shaped structure in which a linear rod was connected to the brush head in solution.

References

1. Wu, J.; Pearce, E. M.; Kwei, T. K.; Lefebvre, A. A.; Balsara, N. P. Macromolecules 2002, 35, 1791.
2. Jenekhe, S. A.; Chen, X. L. Science 1998, 279, 1903.
3. Kukula, H.; Ziener, U.; Schöps, M.; Godt, A. Macromolecules 1998, 31, 5160.
4. Cornelisen, J. J. L.; Fischer, M.; Somerdijk, N. A. J. M.; Nolte, R. J. M. Science 1998, 280, 1427.
5. Sakai, R.; Otsuka, I.; Satoh, T.; Kakuchi, R.; Kaga, H.; Kakuchi, T. J Polym Sci Part A: Polym Chem 2006, 44, 325.
6. Troxell, T. C.; Scheraga, H. A. Macromolecules 1971, 4, 519.
7. Yu, H.; Bur, A. J.; Fetters, L. J. J Chem Phys 1966, 44, 2568.
8. Matyjaszewski, K.; Xia, J. Chem Rev 2001, 101, 2921.
9. Kamigaito, M.; Ando, T.; Sawamoto, M. Chem Rev 2001, 101, 3689.
10. Hawker, C. J.; Bosman, A. W.; Harth, E. Chem Rev 2001, 101, 3661.
11. Chiefari, J.; Rizzardo, E. In Handbook of Radical Polymerization; Matyjaszewski, K.; Davis, T. P., Eds.; Wiley-Interscience: Hoboken, NJ, 2002; p 629.
12. Legge, T. M.; Slark, A. T.; Perrier, S. J Polym Sci Part A: Polym Chem 2006, 44, 6980.
13. Barner-Kowollik, C.; Buback, M.; Charleux, B.; Coote, M. L.; Drache, M.; Fukuda, T.; Goto, A.; Klumperman, B.; Lowe, A. B.; Mcleary, J. B.; Moad, G.; Monteiro, M. J.; Sanderson, R. D.; Tonge, M. P.; Vana, P. J Polym Sci Part A: Polym Chem 2006, 44, 5809.
14. Lai, J. T.; Shea, R. J Polym Sci Part A: Polym Chem 2006, 44, 4298.
15. Ishizu, K.; Hatoyama, N.; Uchida, S. J Polym Sci Part A: Polym Chem 2007, 45, 4037.
16. Borner, H. G.; Beers, K.; Matyjaszewski, K.; Sheiko, S. S.; Möller, M. Macromolecules 2001, 34, 4375.
17. Ishizu, K.; Yamada, H. Macromolecules 2007, 40, 3056.
18. Shipp, D. A.; Wang, J. L.; Matyjaszewski, K. Macromolecules 1998, 31, 8005.
19. Chatterjee, D. P.; Mandal, B. M. Polymer 2006, 47, 1812.
20. Karanam, S.; Gossens, H.; Klumperman, B.; Lemstra, P. Macromolecules 2003, 36, 3051.
21. Neugebauer, D.; Sumerlin, B. S.; Matyjaszewski, K.; Goodhart, B.; Sheiko, S. S. Polymer 2004, 45, 8173.
22. Nemoto, N.; Nagai, M.; Koike, A.; Okada, Y. Macromolecules 1995, 28, 3859.
23. Kawaguchi, H.; Matsumoto, H.; Iriany, H.; Ito, K. Polym Prepr Jpn 1998, 47, 1694.